[redacted] X M 54807 Copy 525
RM E58E14

NACA RM E58E14

19 p.

[redacted] 63 18045
Code-1

RESEARCH MEMORANDUM

PERFORMANCE OF AN ALL-INTERNAL CONICAL COMPRESSION INLET WITH ANNULAR THROAT BLEED AT MACH NUMBER 5.0

By Leonard E. Stitt and Leonard J. Obery

Lewis Flight Propulsion Laboratory
Cleveland, Ohio

CLASSIFICATION CHANGED TO UNCLASSIFIED EFFECTIVE JUNE 12, 1963
AUTHORITY NASA TIB-4 BY J. J. CARROLL

OTS PRICE
XEROX $ 1.60
MICROFILM $ 0.50

[redacted]

NATIONAL ADVISORY COMMITTEE
FOR AERONAUTICS
WASHINGTON
August 6, 1958

[redacted]

DECLASSIFIED

NACA RM E58E14

NATIONAL ADVISORY COMMITTEE FOR AERONAUTICS

RESEARCH MEMORANDUM

PERFORMANCE OF AN ALL-INTERNAL CONICAL COMPRESSION INLET WITH ANNULAR THROAT BLEED AT MACH NUMBER 5.0*

By Leonard E. Stitt and Leonard J. Obery

18045

SUMMARY

An all-internal conical compression inlet with annular bleed at the throat was investigated at Mach 5.0 and zero angle of attack. The minimum contraction ratio of the supersonic diffuser, coincident with a mass-flow ratio of 1.0, was determined to be 0.084 as compared with the isentropic contraction ratio of 0.04 at Mach 5.0. The over-all inlet performance was very sensitive to the amount of annular bleed at the throat because of the extensive boundary layer. For example, the critical recovery varied from 41 percent with 6-percent bleed to 59 percent with 25-percent bleed. Decreasing the spacing between the supersonic and subsonic diffusers increased the critical mass-flow ratio but reduced the range of subcritical mass-flow regulation. A constant-area section was required ahead of the subsonic diffuser in order to obtain reasonable performance. An inlet-engine net-thrust analysis indicated that the optimum performance occurred with from 20- to 25-percent bleed, depending on how the bypassed air was handled.

INTRODUCTION

In order to provide experimental data on the performance of inlets at Mach 5.0, a program has been initiated at the NACA Lewis laboratory to investigate the performance of several inlets, including an all-internal compression inlet. A similar all-internal conical compression inlet was previously investigated at Mach numbers from 2.0 to 3.0 (ref. 1), and the present investigation is an application of this inlet type to a Mach number of 5.0. The inlet was designed with enough flexibility to obtain (1) the minimum contraction ratio for the supersonic diffuser with a mass-flow ratio of 1.0, and (2) the relation between the over-all recovery and the throat boundary-layer removal.

This investigation was conducted in the Lewis 1- by 1-foot variable Reynolds number tunnel at Mach 5.0 and a pressure altitude of 100,000 feet. The Reynolds number, based on an inlet diameter of 1/2 foot, was 1.12×10^6.

*Title, Confidential.

[redacted]

SYMBOLS

A	area
C_F	thrust coefficient
D	drag
d	diameter
F	thrust
M	Mach number
m	mass-flow rate
P	total pressure
P'	Pitot pressure
p	static pressure
S	distance between supersonic and subsonic diffusers
γ	ratio of specific heats
η_k	kinetic-energy efficiency

Subscripts:

b	bleed
id	ideal
s	spillage
t	entrance to subsonic diffuser
x	axial distance
0	entrance to supersonic diffuser
1	exit of supersonic diffuser

2 measuring station at start of subsonic diffusion

3 measuring station at end of subsonic diffusion

APPARATUS AND PROCEDURE

Model Design

The model consisted of two basic components, a supersonic diffuser ahead of a subsonic diffuser.

Supersonic diffuser. - The supersonic diffuser was formed from the internal passage of a frustrum of a 10° cone, with an inlet diameter of 6 inches. The diffuser was opened part way on its centerline forming a door, which was hinged at its leading edge. This door was opened to "start" the supersonic flow through the inlet and then was closed for running, as shown in figures 1(a) and (b). The supersonic diffuser was mounted in the tunnel by means of a horizontal support strut (fig. 2). The actuator for opening and closing the starting door was mounted on this strut and can be seen in figure 1(a).

Subsonic diffuser. - The subsonic diffuser was mounted independently of the supersonic diffuser, and the distance between them was varied by translating the subsonic diffuser in the tunnel. Most of the data presented herein were obtained with a constant-area section ahead of the 12°-included-angle conical expansion, as shown in figure 2. The length of the constant-area section was 0.7 inlet diameter for all cases. The performance of the diffuser with the straight section eliminated was also determined for one configuration. The internal-area variation of the inlet with a diameter ratio of 0.885 is presented in figure 3.

Shrouds. - Two shrouds were investigated to simulate a throat boundary-layer-bleed discharge passage that would be required in an actual inlet. As shown in figure 2(b), the flush shroud was formed by a continuation of the exit surface of the supersonic diffuser. This shroud was then cut out to form the stepped-area shroud. The stepped shroud was similar in appearance and identical in concept to the bleed configuration discussed in reference 1.

Computations

For a given configuration the mass flow was regulated by means of a remotely actuated plug at the exit of the subsonic diffuser. The mass-flow ratio was computed from a measured total-pressure recovery at station 3 and the assumption of isentropic flow to the choked exit area. The total-pressure recovery was calculated from an area-weighted average of 24 Pitot tubes at station 3.

[redacted]

RESULTS AND DISCUSSION

The first phase of the investigation was to determine the performance of the supersonic diffuser alone. The convergent passage half-angle, which was arbitrarily selected at 5°, represents an intuitive compromise between shock losses (function of angle) and friction losses and weight (function of diffuser length). The minimum contraction ratio A_1/A_0 of 0.084 was determined experimentally with the supersonic diffuser capturing a full stream tube. In comparison, the isentropic compression ratio at a Mach number of 5.0 is 0.04.

A Pitot-pressure survey of the flow leaving the supersonic diffuser was taken at a spacing ratio S/d_1 of 0.144, representing one possible location of the entrance to the subsonic diffuser. This survey (fig. 4) indicated that the supersonic diffuser wall boundary layer filled about two-thirds of the exit area. Pitot-pressure recoveries outside the boundary layer ranged from 71 to 80 percent of free-stream total pressure. The decrement in total-pressure recovery in the center of the high-pressure core, also noted in reference 1, was attributed to the coalescence of the supersonic compression waves on the centerline of the supersonic diffuser.

The survey indicates the upper limit of pressure recoveries that might be expected by intercepting the flow leaving the supersonic diffuser with subsonic diffusers of varying entrance diameters. The diameter ratios shown in figure 4 represent the physical size of three of the subsonic diffuser inlets used in this investigation. Subsonic diffusers with bleed discharge directly to free stream (fig. 2(a)) and with entrance diameters from 1.34 to 1.74 inches (diameter ratios of 0.77 to 1.00) were located at the plane of survey, and the results are presented in figure 5. The level of the peak recoveries of the various configurations is near the value that might be expected from an integration of the profile shown in figure 4. Subcritical flow, as evidenced by the performance curves, was accomplished by the movement of the normal shock in the bleed gap S between the two diffusers. Schlieren photographs, showing the inlet at various operating points, are presented in figure 6. The performance curves (fig. 5) indicate the relationship between pressure recovery and annular bleed removal. As expected, the critical recovery increased with increased bleed flow. Critical recovery increased from 41 percent with 6-percent bleed to 59 percent with 25-percent bleed; the maximum recoveries were from 4 to 9 counts higher than critical. The lowest mass-flow ratio shown for each configuration (or the highest total-pressure-recovery point) represents the minimum stable mass flow before the normal shock was expelled through the supersonic diffuser. The configuration with the highest supercritical mass-flow ratio had a simulated flush slot bleed at the throat, since the diameters of the supersonic and subsonic diffusers were equal; that is, $d_t/d_1 = 1.0$.

DECLASSIFIED

The total-pressure distribution at station 2, immediately aft of the constant-area section, was obtained for one of the subsonic-diffuser configurations and is presented in figure 7. The over-all performance of the subsonic-diffuser configuration is reproduced at the top of figure 7 for reference, and profiles are shown for four of the performance points, as indicated. The profile was rather asymmetrical in the supercritical range but became more symmetrical with critical and subcritical inlet operation.

Reference 1 determined that the spacing between the diffusers had an appreciable effect on over-all performance. One configuration was run in this investigation to determine a near-optimum spacing ratio. The spacing ratio S/d_1 is defined as the distance between the supersonic and subsonic diffuser divided by the exit diameter of the supersonic diffuser. Decreasing the spacing ratio (fig. 8) increased the critical mass-flow ratio but, as expected, decreased the range of subcritical mass-flow regulation. In fact, with a spacing ratio of 0.072, the normal shock could not be positioned in the bleed gap, and the peak recovery of this configuration was less than the critical recovery of the other two configurations investiated.

All configurations discussed so far had a constant-area section ahead of the subsonic diffuser (figs. 2 and 3). It was reasoned that if a single normal shock could be positioned ahead of the diffuser, the constant-area section should not be required. This was not the case, however, for, as shown in figure 9, the peak recovery decreased from 60 to approximately 42.5 percent when the constant-area section was eliminated. An inspection of the static-pressure distribution in the diffusers of the preceding configurations indicated, in all cases, a pressure rise in the constant-area section even with what apparently was a normal shock standing in the bleed gap (fig. 6). It thus appears from this investigation that some length of constant area is needed ahead of the subsonic diffuser. However, no attempt was made herein to determine an optimum length. Such studies have been conducted elsewhere (e.g., ref. 2).

The configurations presented to this point have all had an immediate bleed discharge to the free stream as indicated in figure 2(a). Obviously, an actual inlet configuration would require a boundary-layer-bleed passage to carry the bleed air to the inlet external surface and then to discharge it rearward. Two shrouded configurations were investigated to simulate a reasonable bleed passage. With a flush shroud, formed by a continuation of the supersonic-diffuser exit (fig. 2(b)), it was found that the normal shock could not be positioned in the bleed gap. Consequently, the peak recovery of this configuration was obtained at critical flow (fig. 10), and no subcritical mass-flow regulation was possible. A step-area change in the shroud, as conceived and reported in reference 1, allowed the normal shock to stand in the bleed gap, and the performance was essentially the same as that of the no-shroud configuration.

Before the drag associated with bypassing air around the throat can be estimated, the recovery level of the bleed air must be determined. A total-pressure survey was made in the annular bleed duct as indicated in the sketch in figure 11. The static- and Pitot-pressure measurements indicated a local Mach number of about 2.9 at this survey plane, resulting in an average bleed recovery of 15 percent of free-stream total pressure when the Pitot-tube readings were corrected for the local normal-shock losses.

A hypothetical inlet-engine net-thrust analysis has been made to obtain the relation between annular bleed flow and optimum inlet thrust minus drag. Five inlets, each with a spacing ratio of 0.144 (fig. 5), were matched to a given engine at two points on each performance curve: (1) critical mass-flow ratio (solid symbols) and (2) minimum stable mass-flow ratio (or peak recovery). The following engine assumptions were made: (a) matching Mach number M_3 of 0.20, (b) thrust coefficient for 100-percent inlet recovery $C_{F_{id}}$ of 10.0 based on engine area, and (c) thrust coefficient, based on free-stream-tube area, for any inlet total-pressure recovery computed from

$$C_F = 2\left(1.6\sqrt{\eta_k} - 1\right)$$

where

$$\eta_k = 1 - \frac{2}{(\gamma-1)M_0^2}\left[\left(\frac{1}{P_3/P_0}\right)^{\frac{\gamma-1}{\gamma}} - 1\right]$$

The computation of spillage drag D_s was based on the following assumptions: (1) All the reduction in engine mass-flow ratio was accomplished by an annular bypass at the inlet throat, (2) the bypass discharge was assumed to be in an axial direction, (3) the bypass exit total-pressure recovery was assumed to be 15 percent, and (4) bypass drag coefficients were computed for a sonic exit area and for an exit area that expanded the flow to free-stream static pressure or an exit Mach number of 3.6.

The results of this analysis are presented in figure 12. The inlet efficiencies were highest when the bleed flow was expanded to p_0, as expected. For sonic discharge the optimum performance was obtained with about 20-percent bleed flow. This corresponds to the configuration with a diameter ratio of 0.828 in figure 5. The bleed-drag coefficient for 20-percent spillage was about 0.10, based on inlet area. When the bleed flow was expanded to free-stream static pressure, the optimum inlet performance was obtained with higher bleed flows (fig. 12(b)). The spillage drag coefficient for 25-percent bleed was about 0.03 in this case. It should be pointed out that the spillage drags for the two methods of

RESTRICTED

exhausting bypass flow (fig. 12) probably represent the maximum and minimum values, respectively, that would be obtained for the conditions stated. In a practical case, the spillage drag would probably fall in between the two cases shown.

SUMMARY OF RESULTS

The following results were obtained with an all-internal conical compression inlet with annular throat bleed at a Mach number of 5.0:

1. The minimum contraction ratio for the supersonic diffuser, with a mass-flow ratio of 1.0, was determined to be 0.084 as compared with the isentropic compression ratio of 0.04 at this Mach number.

2. Critical total-pressure recoveries varied from 41 to 59 percent with 6- and 25-percent bleed, respectively. Peak total-pressure recoveries were from 4 to 9 counts higher than critical.

3. As the spacing between the supersonic and subsonic diffusers was decreased, (a) the critical mass-flow ratio was increased and, as expected, the range of subcritical mass-flow regulation was decreased, and (b) a minimum spacing ratio was obtained where the normal shock could not be positioned in the bleed gap.

4. Eliminating the constant-area section ahead of the subsonic diffuser decreased the peak recovery from 60 to approximately 42.5 percent.

5. Optimum inlet efficiency was obtained with about 20- to 25-percent boundary-layer-bleed flow, depending on the method of discharging the bypassed air.

Lewis Flight Propulsion Laboratory
National Advisory Committee for Aeronautics
Cleveland, Ohio, May 27, 1958

REFERENCES

1. Luidens, Roger W., and Flaherty, Richard J.: Use of a Shock-Trap Bleed to Improve the Pressure Recovery of Fixed- and Variable-Capture-Area Internal-Contraction Inlets; Mach Number 2.0 to 3.0. NACA RM E58D24, 1958.

2. McLafferty, G. H., et al.: Investigation of Turbojet Inlet Design Parameters. R-0790-13, United Aircraft Corp., Dec. 1955. (Dept. Navy, Bur. Aero. Contract NOas 55-133-c.)

[redacted]

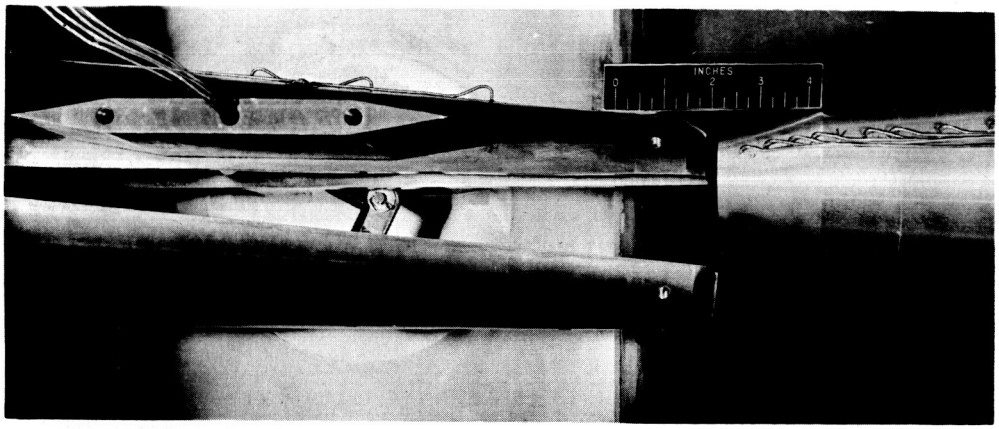

M_0 →

C-46414

(a) Door open for starting.

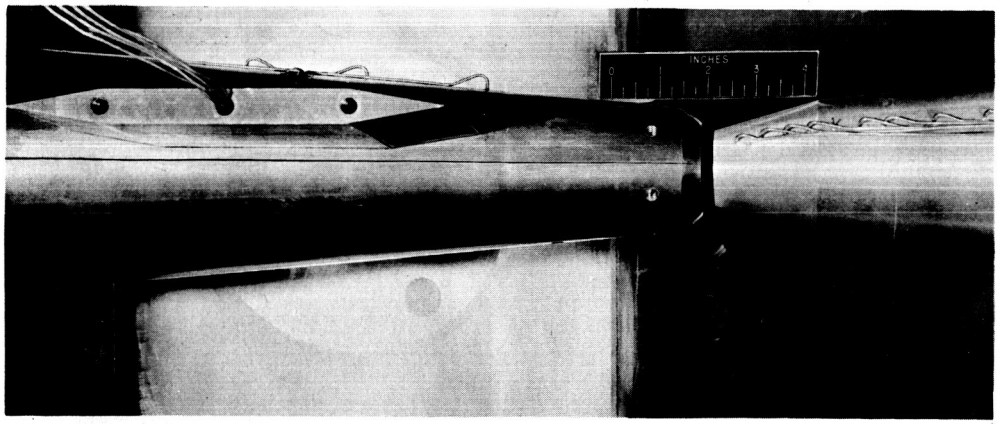

M_0 →

C-46413

(b) Running position.

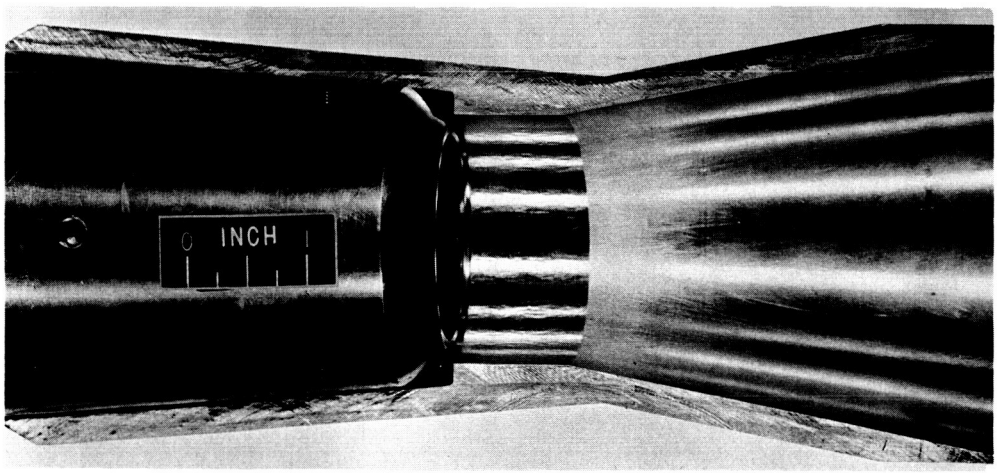

M_0 →

(c) Stepped shroud.

C-46751

Figure 1. - Supersonic diffuser.

UNCLASSIFIED

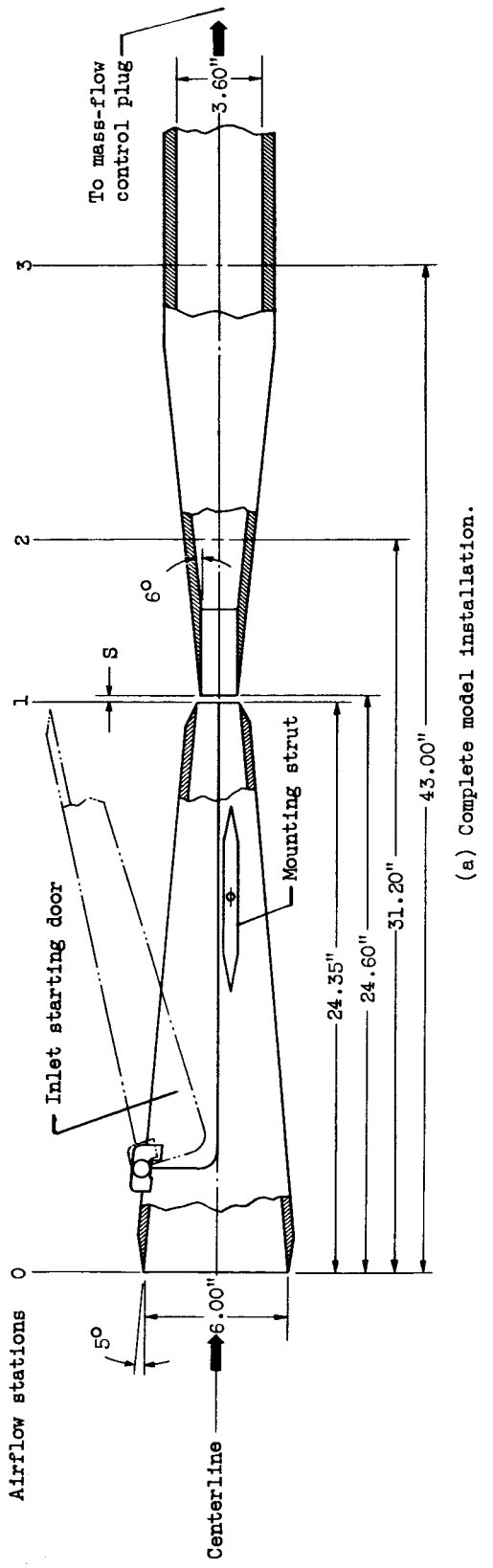

(a) Complete model installation.

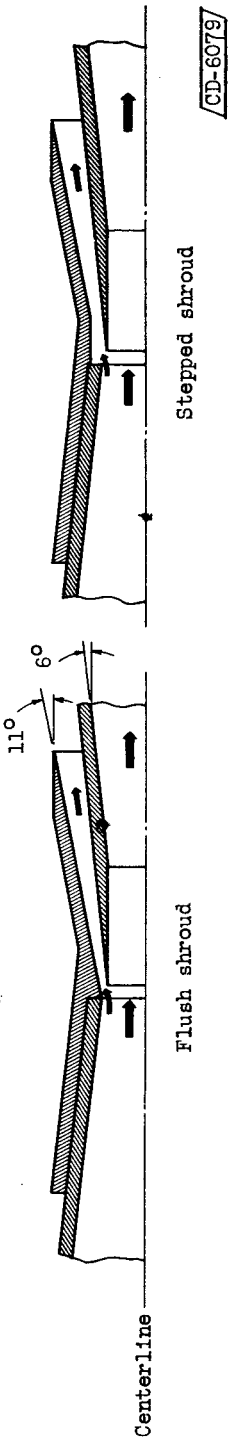

(b) Types of boundary-layer-bleed passages.

Figure 2. - Supersonic and subsonic diffuser details.

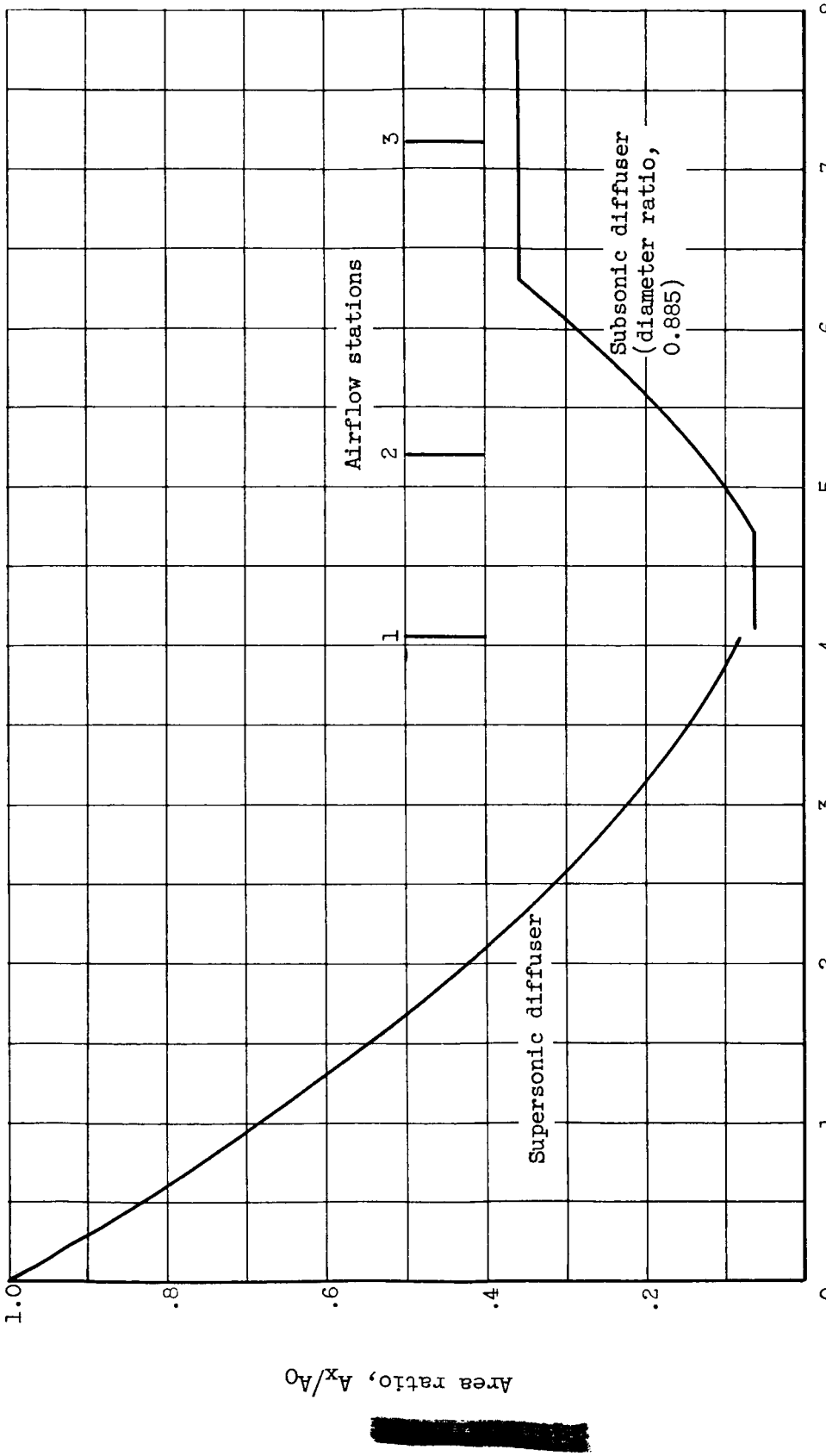

Figure 3. - Internal area variation. Inlet capture area, A_0, 28.3 square inches; inlet diameter, d_0, 6 inches.

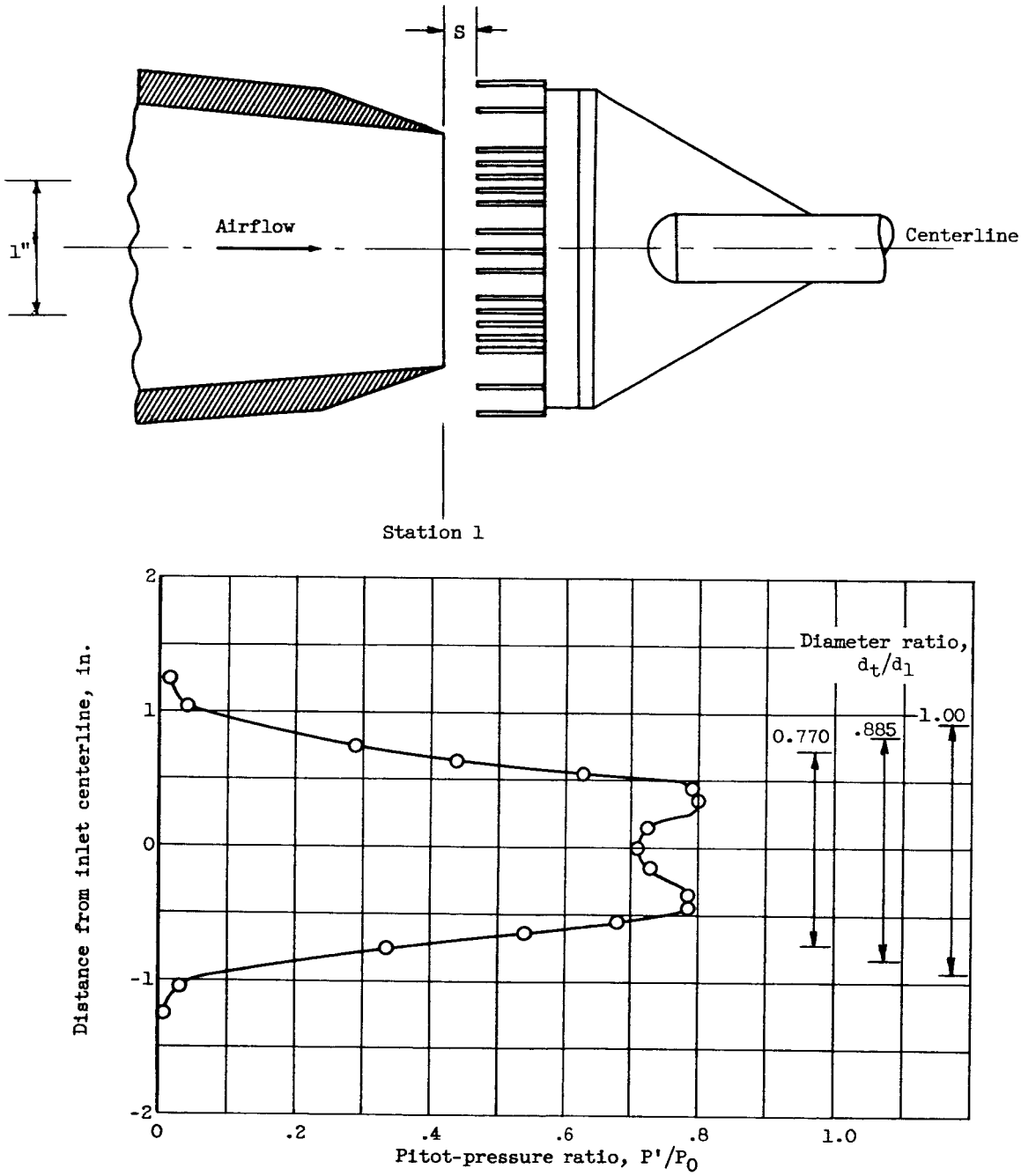

Figure 4. - Pitot-pressure survey of flow leaving supersonic diffuser. Survey plane at spacing ratio, S/d_1, of 0.144. Supersonic-diffuser contraction ratio, A_1/A_0, 0.084.

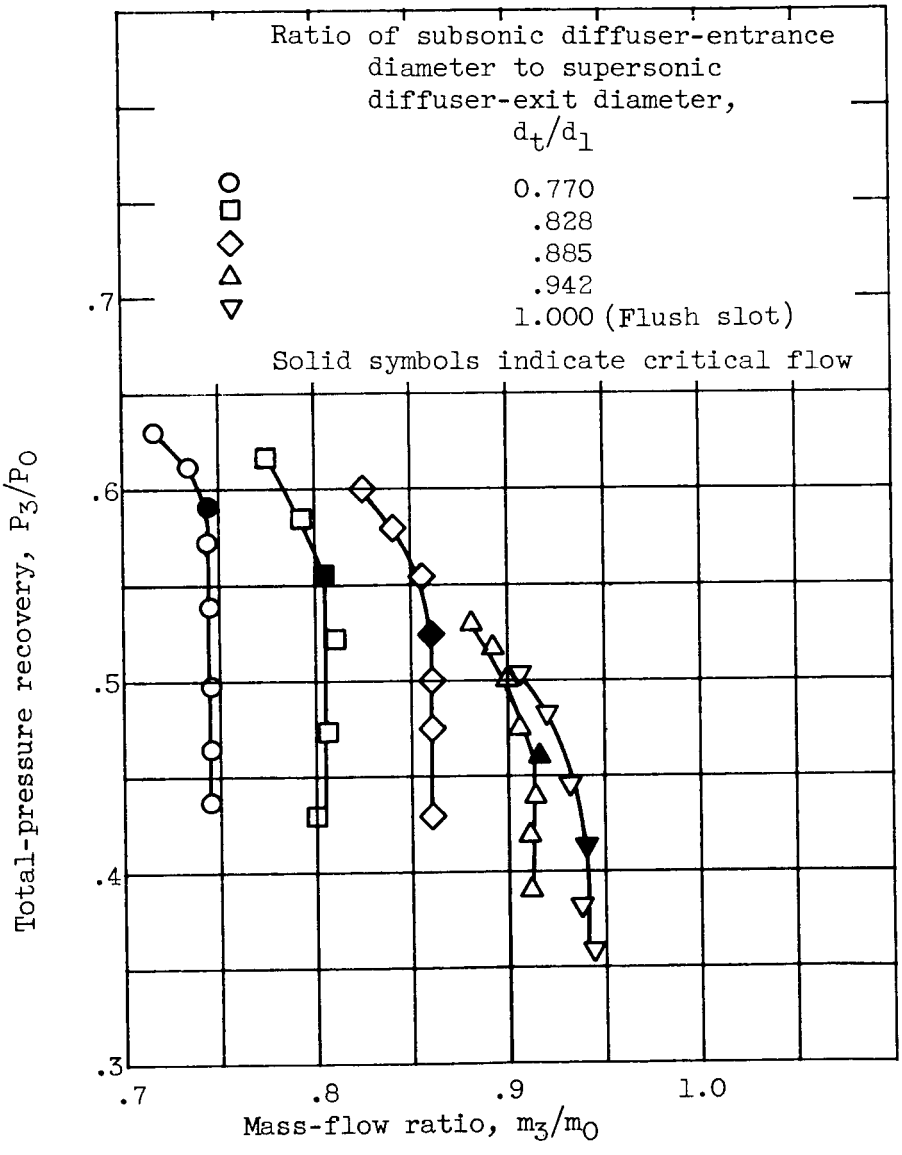

Figure 5. - Effect of increasing subsonic-diffuser entrance area. Spacing ratio, S/d_1, 0.144.

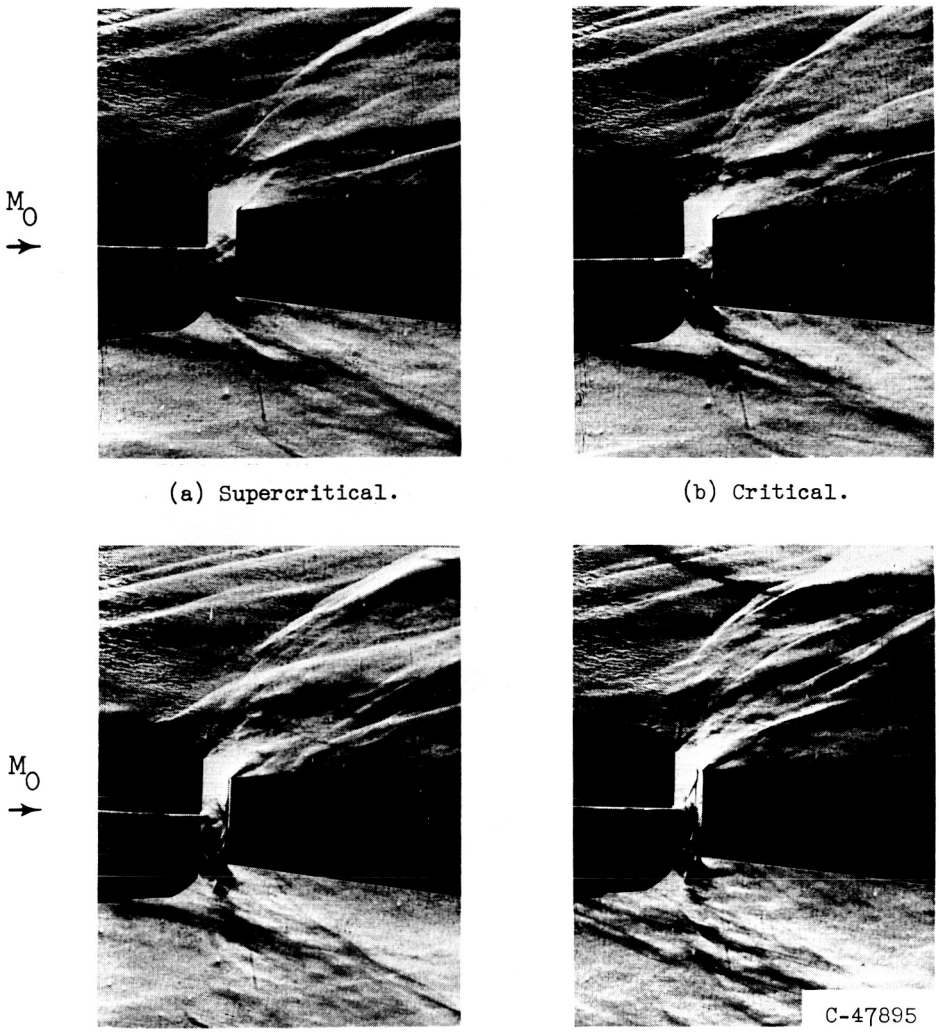

(a) Supercritical. (b) Critical.

(c) Subcritical. (d) Minimum stable.

Figure 6. - Normal-shock position in bleed gap. Spacing ratio, S/d_1, 0.288; diameter ratio, d_t/d_1, 0.770.

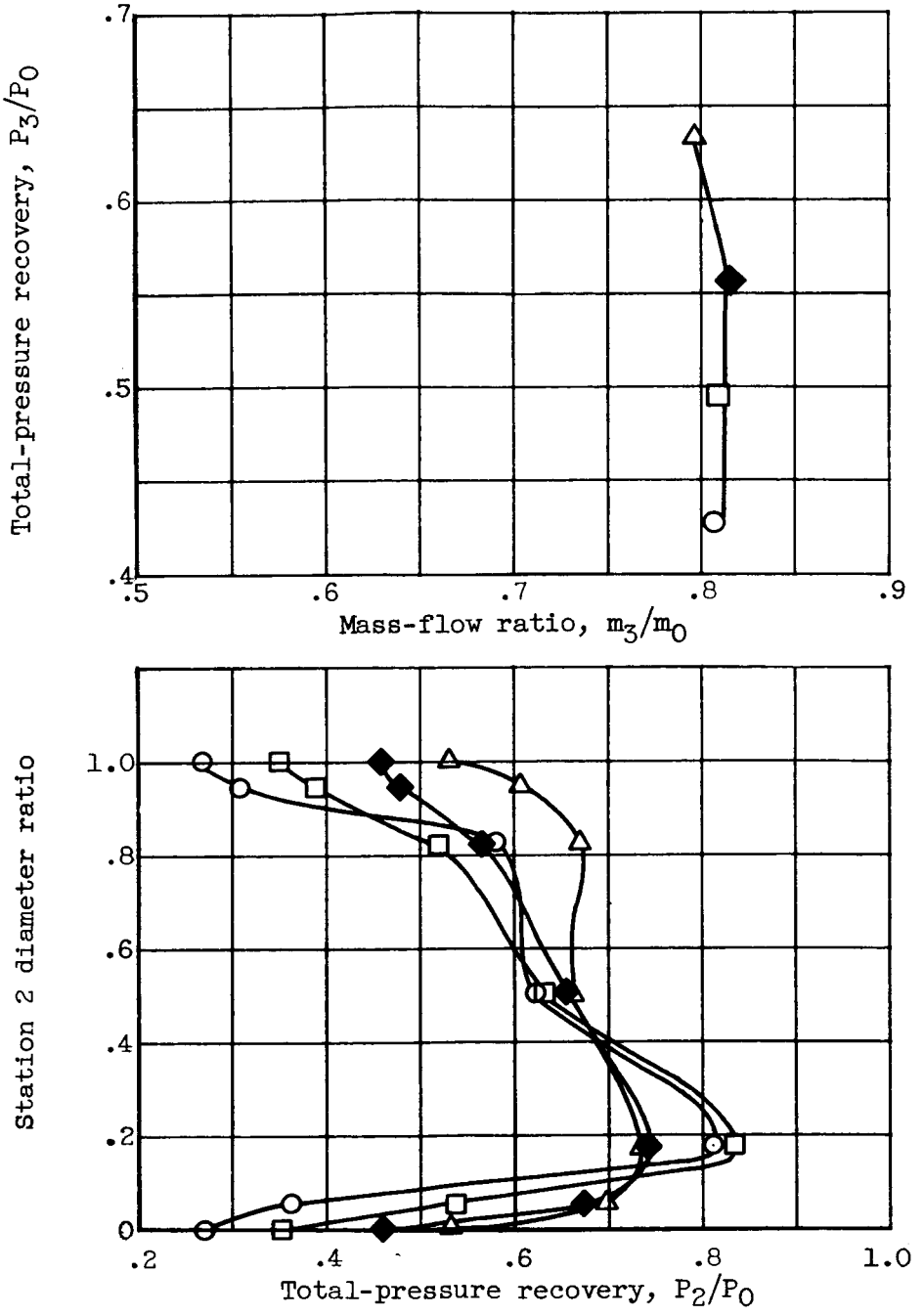

Figure 7. - Total-pressure-recovery profiles at station 2. Spacing ratio, S/d_1, 0.144; diameter ratio, d_t/d_1, 0.828.

DECLASSIFIED

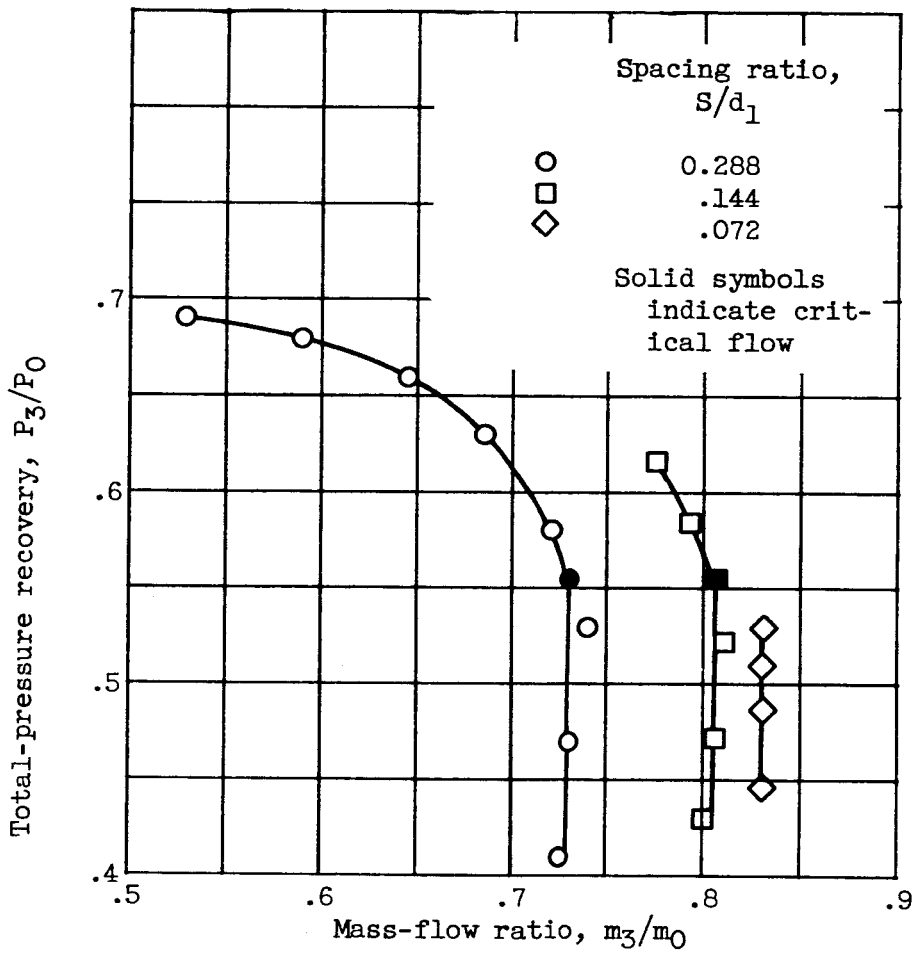

Figure 8. - Effect of spacing ratio. Diameter ratio, d_t/d_1, 0.828.

Figure 10. - Effect of shrouding inlet throat. Spacing ratio, S/d_1, 0.144; diameter ratio, d_t/d_1, 0.828.

Figure 9. - Effect of constant-area section at throat of subsonic diffuser. Spacing ratio, S/d_1, 0.144; diameter ratio, d_t/d_1, 0.885.

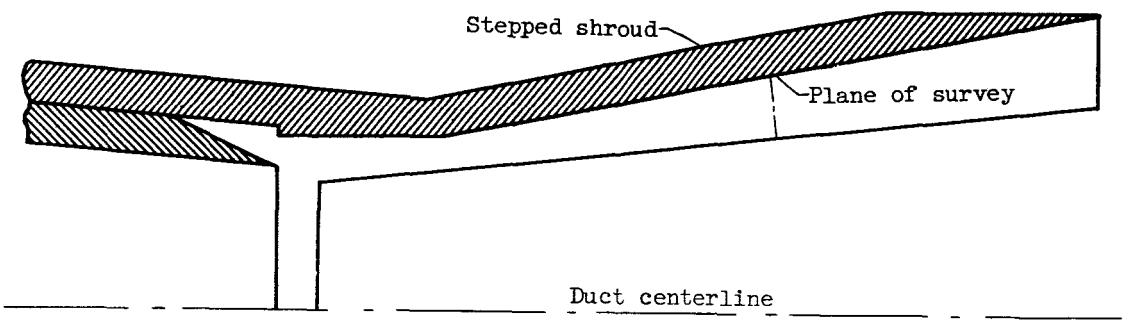

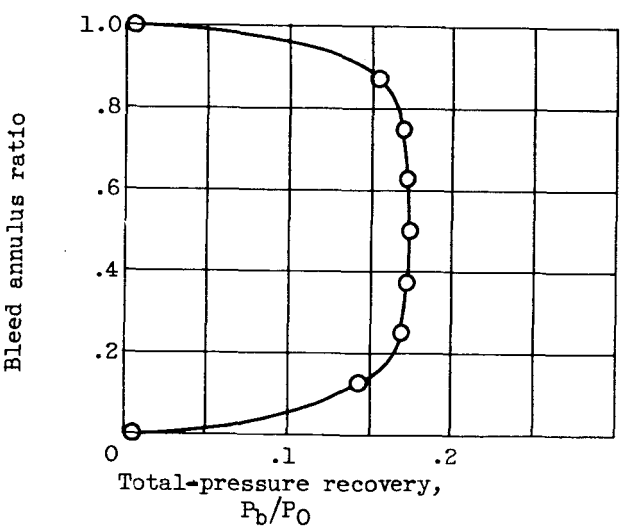

Figure 11. - Total-pressure-recovery profile for annular bleed duct. Spacing ratio, S/d_1, 0.144; diameter ratio, d_t/d_1, 0.885.

[redacted]

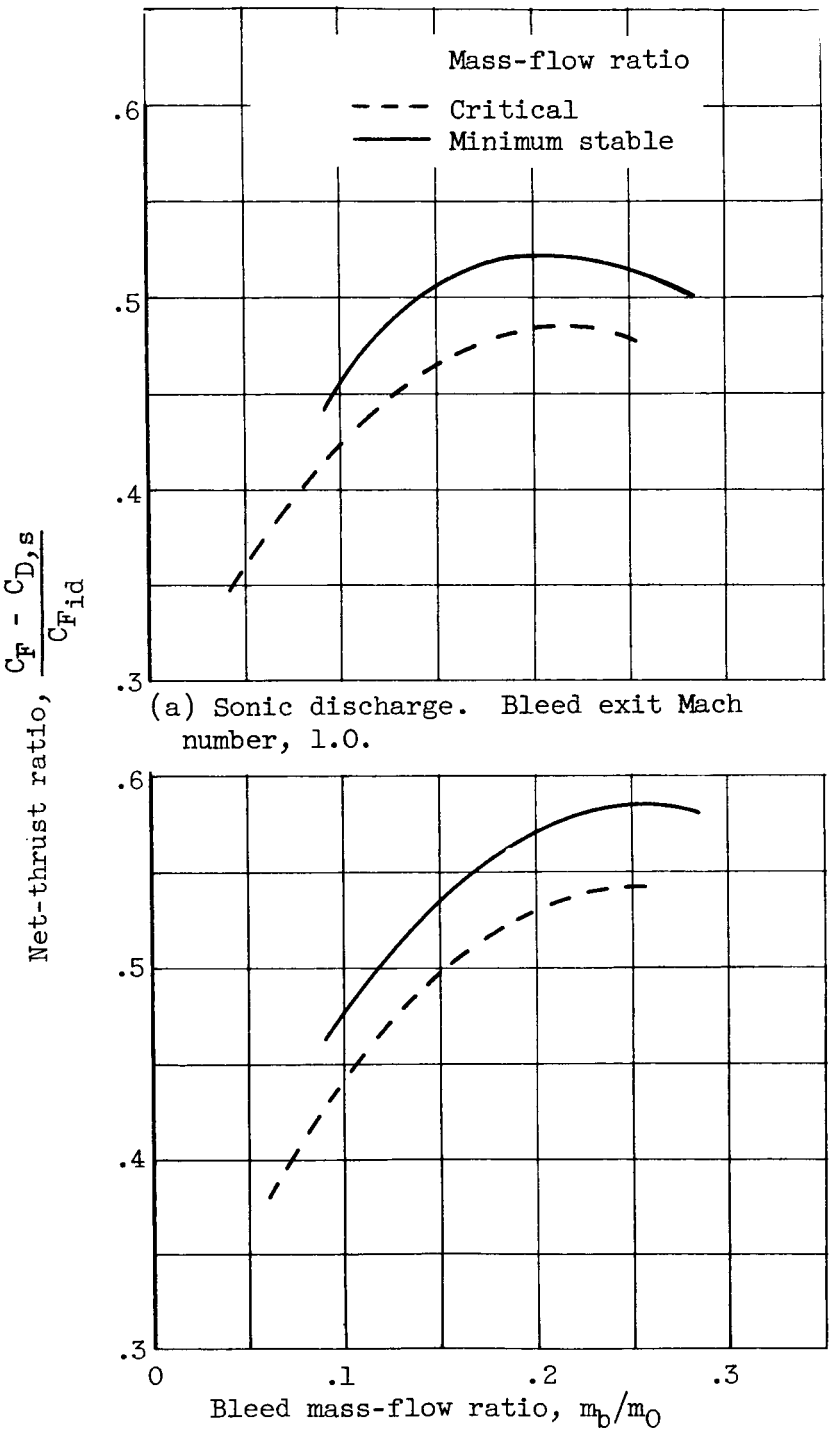

(a) Sonic discharge. Bleed exit Mach number, 1.0.

(b) Bleed flow expanded to free-stream static pressure, p_0. Bleed exit Mach number, 3.6.

Figure 12. - Inlet-engine net-thrust analysis. [redacted]